TÜBİTAK

Turkish Journal of Chemistry

http://journals.tubitak.gov.tr/chem/

Research Article

Turk J Chem
(2018) 42: 1755 – 1767
© TÜBİTAK
doi:10.3906/kim-1801-58

Determination of hydrogen peroxide with an enzymeless amperometric sensor based on poly(vinylferrocene)-supported Ag nanoparticles

Mutlu SÖNMEZ ÇELEBİ*, Kübra ÖZTÜRK, Mehmet DUMANGÖZ, Filiz KURALAY
Department of Chemistry, Faculty of Science and Arts, Ordu University, Ordu, Turkey

Received: 19.01.2018 • **Accepted/Published Online:** 03.07.2018 • **Final Version:** 06.12.2018

Abstract: An enzymeless electrochemical sensor for detection of low amounts of H_2O_2 with the aid of Ag nanoparticles supported on conducting poly(vinylferrocene) (PVF) film was developed. Experimental results revealed that contribution of Ag nanoparticles led to remarkable improvement by means of reduction potential and reduction current. Influence of experimental parameters (i.e. polymeric film thickness, concentration of Ag precursor, immersion time in precursor solution, reduction time, and reduction potential) were investigated. The Ag/PVF-modified electrode system was characterized physically by scanning electron microscopy. The results revealed that the sensor developed was easy-to-prepare, economic, selective, and sensitive, with a fast response time of 3 s. The linear concentration range of the sensor was 0.1–50 mM, with a sensitivity of 14.1 μA mM^{-1} and a limit of detection of 0.94 μM. Finally, interference effects of uric acid, ascorbic acid, dopamine, and glucose molecules were studied and no significant interference was observed at physiological levels.

Key words: Hydrogen peroxide determination, electrochemical sensor, poly(vinylferrocene), silver nanoparticles, modified electrode

1. Introduction

Hydrogen peroxide (H_2O_2)-a very small compound in nature—is an interesting molecule because of its importance in both industrial processes and biological processes. It is not only involved in many processes such as food processing, textile industry, pulp and paper bleaching, and minerals processing, but also utilized in diverse areas such as pharmaceutical research and organic synthesis.[1,2] It is even used as an oxidant in fuel cell systems. Last but not least, it is the by-product of several reactions that involve enzymes such as glucose oxidase, cholesterol oxidase, and lactate oxidase. It is also a substrate for the enzyme horseradish peroxidase. Therefore, the reliable, accurate, sensitive, rapid, and low-cost determination of H_2O_2 has been practically important and widely investigated.

Conventional techniques for H_2O_2 determination, such as chemilumimescence,[3,4] fluorescence,[5,6] and spectrophotometry[7,8] are complex, costly, and time-consuming. In comparison, electrochemistry can offer simple, rapid, sensitive, and cost-effective means, since H_2O_2 is an electroactive molecule.[9,10] However, electrochemical applications are limited by slow electrode kinetics, high overpotential, and possible interferences from other existing electroactive species in real samples. Thus, current research on electrochemical H_2O_2 detection is mainly focused on electrode modifications in order to decrease the overpotential and increase the electron

*Correspondence: mutlucelebi@odu.edu.tr

transfer kinetics.[11] For these considerations, a large range of materials such as redox proteins,[12] dyes,[13] transition metals,[14] metal oxides,[15] redox polymers,[16] and carbon nanotubes[17] are studied. On the other hand, in recent years, nanomaterials, especially nanoparticles, have been successfully applied to electrochemical sensors improving the sensitivity of the sensor due to large surface area and porous structure leading to a decrease in the overpotential for many analytes.[18,19]

The main objective of the current study was to prepare an enzymeless electrochemical sensor for detection of low amounts of H_2O_2 with the aid of Ag nanoparticles supported on conducting poly(vinylferrocene) (PVF) film. Recently, the relatively high cost and lack of long-term stability of enzyme biosensors has led to an effort to develop new sensors that mimic the function of enzymes. Avoiding use of an enzyme during the construction of a sensor is also encouraged because of the lack of protein denaturation and subsequent decrease in sensitivity. For these purposes, nanoparticles are considered excellent substitutes for enzymes.[20,21] Many nanoparticle-based electrochemical H_2O_2 sensors have been reported in the literature, including Ag,[22,23] Au,[24,25] Pt,[26,27] and Pd.[28,29] Among these, Ag nanoparticles have been successfully applied as an effective catalyst for amperometric H_2O_2 detection without use of an enzyme. Ag nanoparticles are known to be responsible for the sensor response due to the electrochemical reduction of H_2O_2.[30,31] Moreover, many forms of nano-sized Ag have been found effective for H_2O_2 sensing.[32–40]

In the present work, a modified electrode system was developed and used as the working electrode of an amperometric H_2O_2 sensor. PVF, a redox polymer, was used as support material on a Au electrode for incorporation of Ag nanoparticles, with a view to combine the features of PVF and Ag nanoparticles for enhanced sensor response. To the best of our knowledge, this is the first study that combines use of Ag nanoparticles with PVF polymer, and the sensor has the advantage of easy preparation together with a low limit of detection (LOD) compared with similar studies in the literature. One of the most important benefits of using PVF is the ease of modification of the electrode and control of the modification parameters during the procedure. It is well known from previous studies that PVF provides an excellent medium for biological compounds and has been employed in many electrochemical sensors.[41–49] In order to obtain maximum current for H_2O_2 reduction, the influence of experimental parameters was investigated. The Ag/PVF modified electrode system was characterized physically by scanning electron microscopy (SEM).

2. Results and discussion

PVF-supported Ag nanoparticles were prepared following a very simple, three-step procedure: (i) coating the Au electrode with polymer film, (ii) immersion of the film coated electrode in aqueous solution of Ag^+ at open circuit, (iii) electrochemical reduction of Ag^+ ions by constant potential electrolysis.

During the procedure, the polymer film was deposited onto the working electrode by electrooxidation of methylene chloride solution of PVF containing tetra-n-butylammonium perchloride (TBAP) as the supporting electrolyte. The thickness of the polymer film was controlled by the charge passed during electrolysis. As an example, a charge of 1×10^{-3} C corresponds to 1.32×10^{-6} mol of the oxidized PVF per cm^2 (dry thickness of approximately 300 μm, which corresponds to about 3×10^5 layers).[50] The resulting film has a porous structure containing ClO_4^- ions as the counter ion, ferrocene, and ferrocenium groups.[51] From previous experience, we know that the PVF-coated electrode is readily capable of immobilizing Ag^+ ions from an aqueous solution.[52] Therefore, in the second step, the PVF-coated electrode was immersed in a stirred aqueous solution of $AgNO_3$ in order to immobilize the Ag^+ ions in the polymeric matrix prior to electrochemical reduction at constant

potential to obtain PVF-supported Ag nanoparticles. The resulting Ag/PVF coated electrode was used as an enzymeless sensor for H_2O_2 detection.

In order to evaluate the influence of Ag nanoparticles on the response of the modified electrode system towards H_2O_2 reduction, cyclic voltammograms (CVs) of H_2O_2 solution were recorded and compared with those of an uncoated Au electrode, a PVF-coated Au electrode, and the Ag/PVF modified Au electrode (Figure 1). In the uncoated Au and PVF-coated Au electrodes, reduction of H_2O_2 was observed to a smaller extent at higher potentials (Figures 1a and 1b). However, when the PVF-coated electrode was decorated with Ag nanoparticles, both the reduction potential and the reduction peak current values were improved considerably (Figure 1c). CVs recorded with the Ag/PVF modified Au electrode in N_2-saturated phosphate buffer system (PBS, pH = 7.0) in the absence and presence of 1.0 mM H_2O_2 are also presented as an inset in Figure 1.

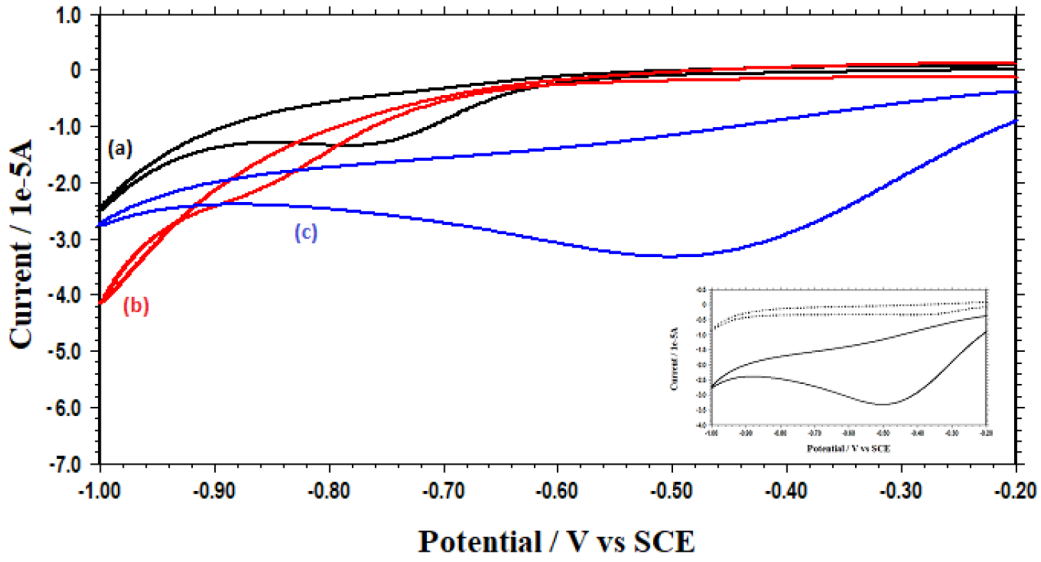

Figure 1. CVs recorded with (a) uncoated Au electrode, (b) PVF-coated Au electrode, (c) Ag/PVF-modified Au electrode in N_2-saturated PBS (pH = 7.0) in the presence of 1.0 mM H_2O_2. Inset: CVs recorded with Ag/PVF-modified Au electrode in N_2-saturated PBS (pH = 7.0) in the absence ($\cdots$ and presence ($-$) of 1.0 mM H_2O_2. Scan rate: 100 mV s^{-1}.

The effect of scan rate during electrocatalytic reduction of H_2O_2 with the Ag/PVF-modified Au electrode was investigated. As seen from the CVs in Figure 2a, cathodic peak potential shifts gradually towards negative potentials as the scan rate increases, which confirms kinetic limitation in the electrochemical reaction. Additionally, a plot of peak current versus the square root of scan rate ($v^{1/2}$) displayed a linear relationship, indicating that the process is diffusion-controlled rather than surface-controlled (Figure 2b).

2.1. Optimization of experimental parameters

Several experimental parameters, such as polymeric film thickness and $AgNO_3$ concentration, were investigated to obtain the maximum peak current for H_2O_2 reduction for best sensor response. Optimization of these parameters was performed according to the reduction peak current values recorded during CVs of 1.0 mM H_2O_2 in 50 mM PBS buffer (pH = 7.0).

Thickness of the polymer coating on the working electrode is an important parameter because it affects the porosity of the polymer film. As mentioned above, the thickness of the polymer film was controlled by the

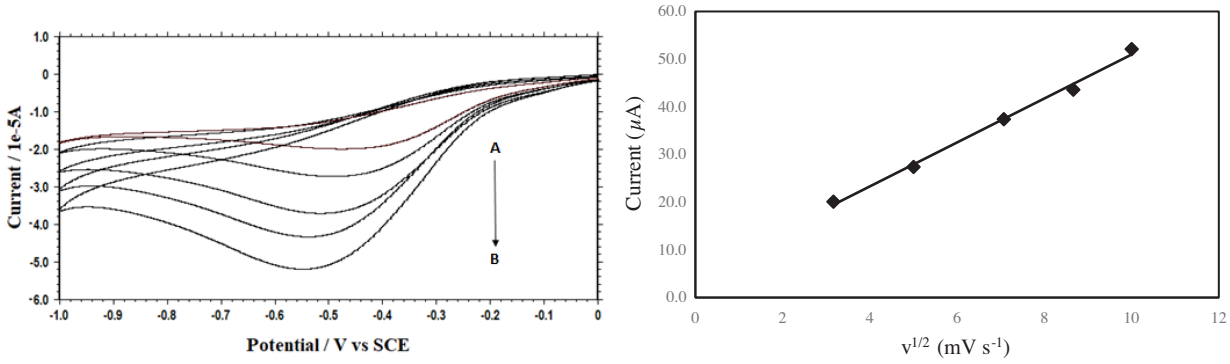

(a) (b)

Figure 2. (a) CVs recorded with Ag/PVF-modified Au electrode in N_2-saturated PBS (pH = 7.0) in the presence of 5.0 mM H_2O_2 at different scan rates: (A) 10, (B) 25, (C) 50, (D) 75, and (E) 100 mV s^{-1}. (b) Plot of peak potential versus square root of scan rate.

charge passed during electrolysis. To evaluate the influence of polymer film thickness, PVF films of different thicknesses were coated on the working electrode and immersed in stirred 1.0 mM $AgNO_3$ solution for 10 min. The electrode was then washed with distilled water and transferred into a cell containing 50 mM PBS (pH = 7.0). Then constant potential electrolysis was applied at –0.2 V (versus saturated calomel electrodes [SCE]) for 300 s in order to reduce the adsorbed Ag^+ ions to metallic Ag, and CVs of H_2O_2 solution were recorded and compared. Polymer film corresponding to 3.0 mC showed the best performance and therefore the optimum thickness was determined (Figure 3a).

Concentration of $AgNO_3$ solution was also an important parameter that probably controlled the size of the Ag nanoparticles, along with the immersion time in Ag^+ solution. We studied with Ag^+ solutions within the concentration range 1.0 to 6.0 mM, keeping all other parameters constant throughout the trials (3.0 mC charge passed during polymer coating, 10 min immersion time in Ag^+ solution, 300 s electrolysis at –0.2 V versus SCE). As can be seen from Figure 3b, H_2O_2 reduction peak current was significantly higher for the 4.0 mM $AgNO_3$ solution. We also studied the influence of immersion time in stirred $AgNO_3$ solution and obtained a maximum at 15 min for H_2O_2 reduction peak current (Figure 3c).

Probably the most outstanding feature of our work is the ease of the nanoparticle synthesis compared with similar studies in the literature, because synthesis of metal nanoparticles generally requires complex and time-consuming procedures. However, we managed to obtain Ag nanoparticles dispersed on the PVF matrix simply by using bulk electrolysis at moderate potentials through electroreduction of the adsorbed ionic species. After immobilizing Ag^+ ions in the polymer matrix via a simple dip-coating process, we applied constant potential electrolysis in 50 mM PBS (pH = 7.0) to obtain Ag nanoparticles. According to the experimental results, only 4 min of electrolysis at –0.2 V (versus SCE) was enough to obtain improved catalytic activity from the Ag/PVF system towards H_2O_2 reduction (Figures 3d and 3e).

2.2. Physical characterization of the modified electrode

The morphology and structure of the polymer film before and after incorporation of Ag nanoparticles were characterized by SEM. For SEM studies, the modified electrode system was prepared using pencil graphite electrodes (PGEs) with identical surface area. As clearly seen in Figure 4a, the polymer film has a porous structure that supports adsorption of the Ag^+ ions, and the Ag nanoparticles are well dispersed in the polymeric

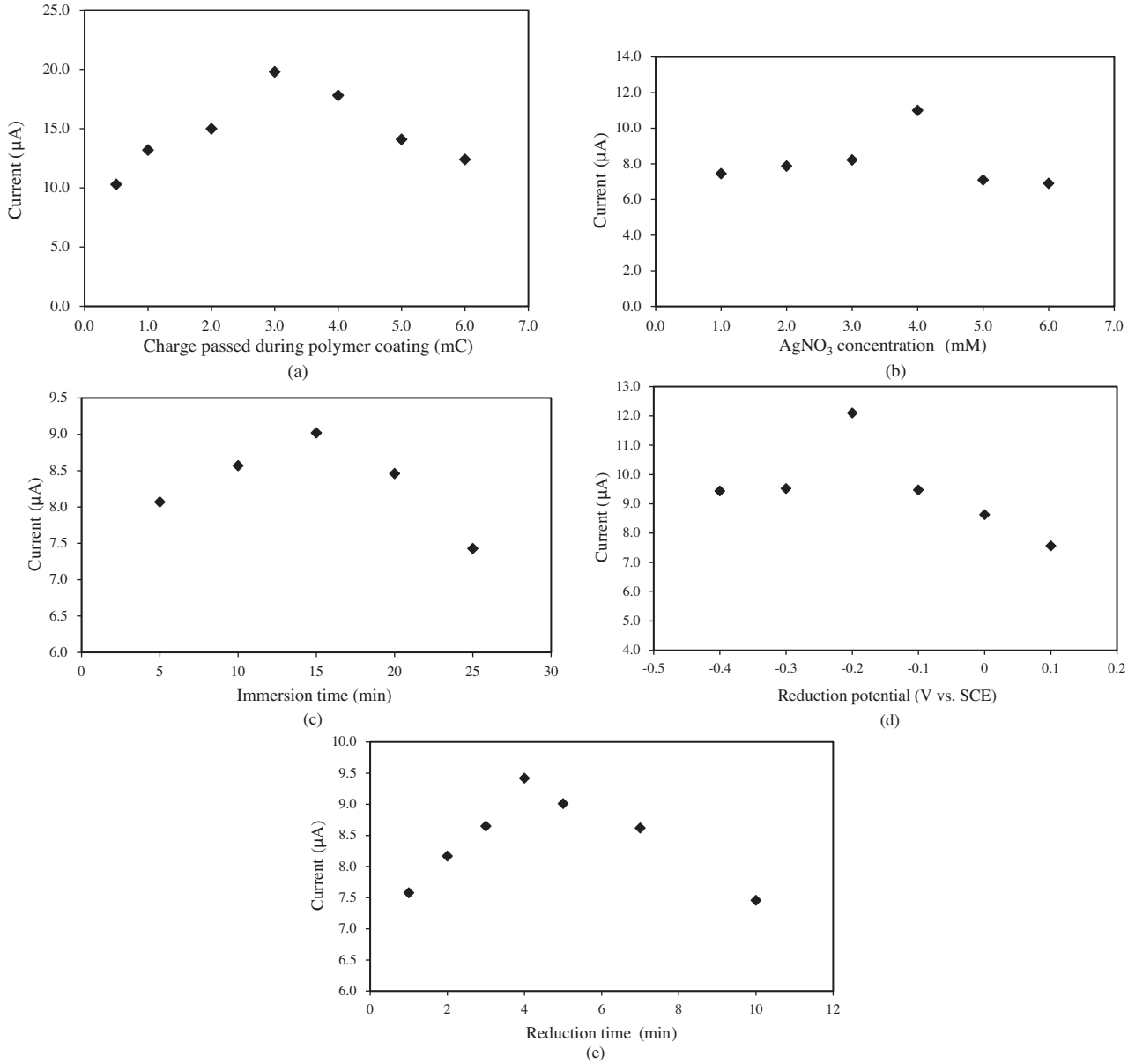

Figure 3. Influence of experimental parameters on reduction peak current of H_2O_2 (a) polymeric film thickness, (b) $AgNO_3$ concentration, (c) immersion time in $AgNO_3$, (d) reduction potential of Ag^+ ions, (d) reduction time of Ag^+ ions. (Data obtained from CVs of N_2-saturated PBS (pH = 7.0) in the presence of 1.0 mM H_2O_2.)

matrix (Figure 4b) with an average particle size of 12 nm. The corresponding energy-dispersive X-ray (EDX) spectra of the PVF film before and after incorporation of Ag nanoparticles and the elemental mapping of the Ag/PVF catalyst system is presented in Figures 4c and 4d, indicating the presence of Ag atoms well dispersed in the polymer matrix.

2.3. Effect of pH

In order to apply the modified electrode to amperometric H_2O_2 detection, we controlled the catalytic activity of the Ag/PVF system towards H_2O_2 reduction at the physiological pH (7.4). For this purpose, we studied

the effect of pH of the H_2O_2 solution on the response of the Ag/PVF modified electrode, which was prepared at the optimum conditions. It is clearly seen from Figure 5 that the activity was highest at around pH 7.0 and was also active between pH values 7.0 and 7.5.

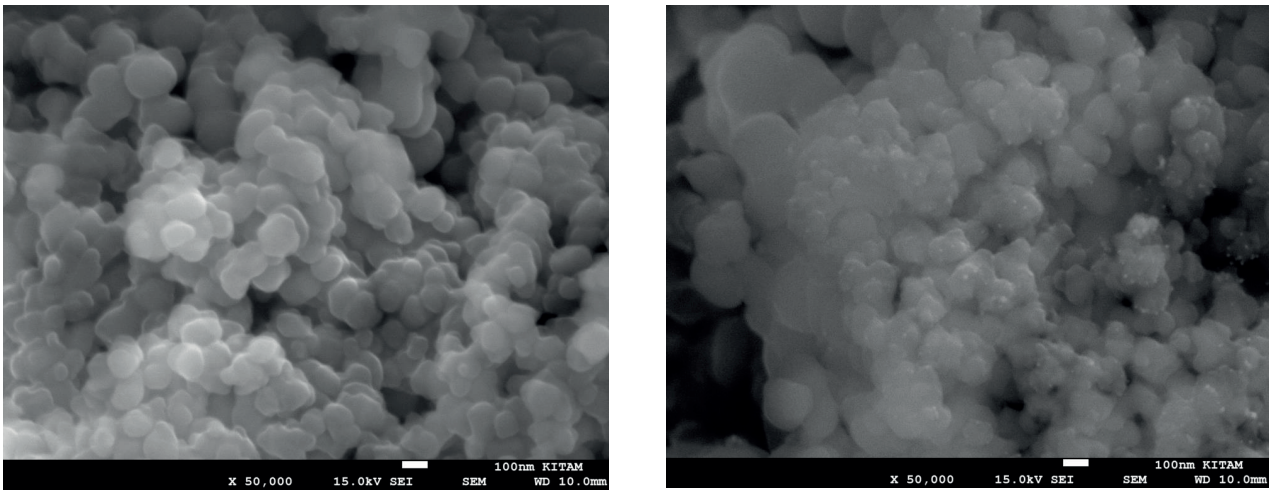

(a) (b)

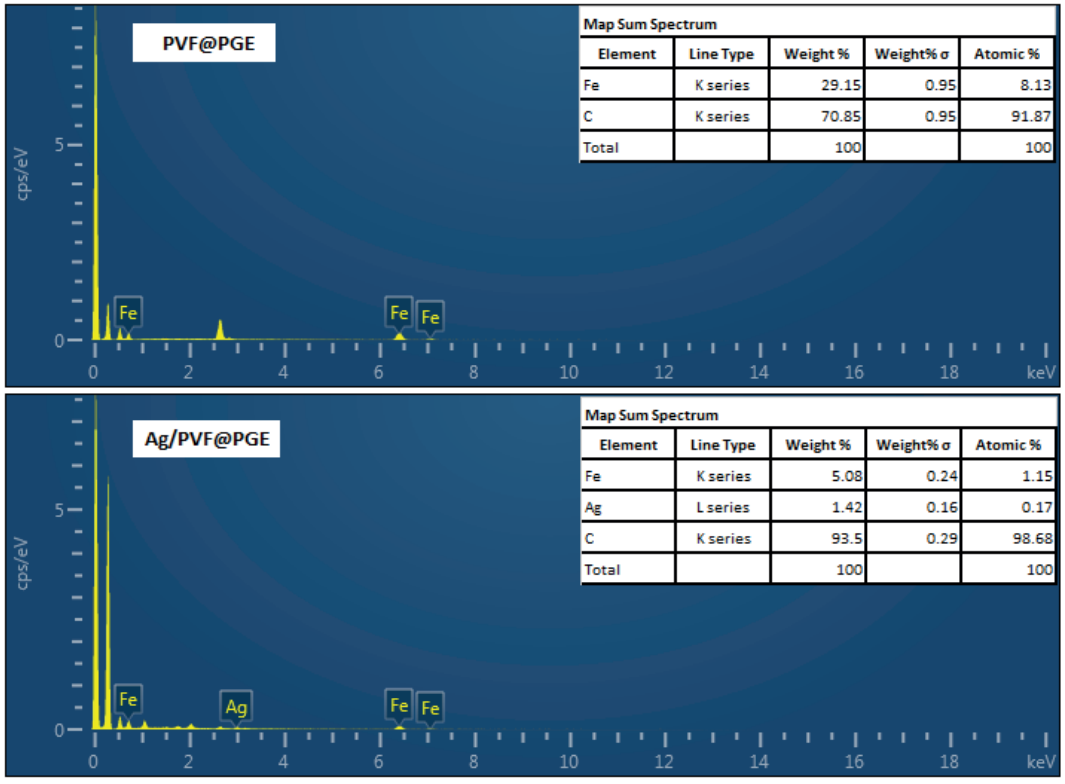

(c)

Figure 4. SEM images of (a) PVF-modified, (b) Ag/PVF-modified PGE. (c) EDX spectra and composition of PVF- and Ag/PVF-modified PGE. (d) Elemental mapping of Ag/PVF-modified PGE.

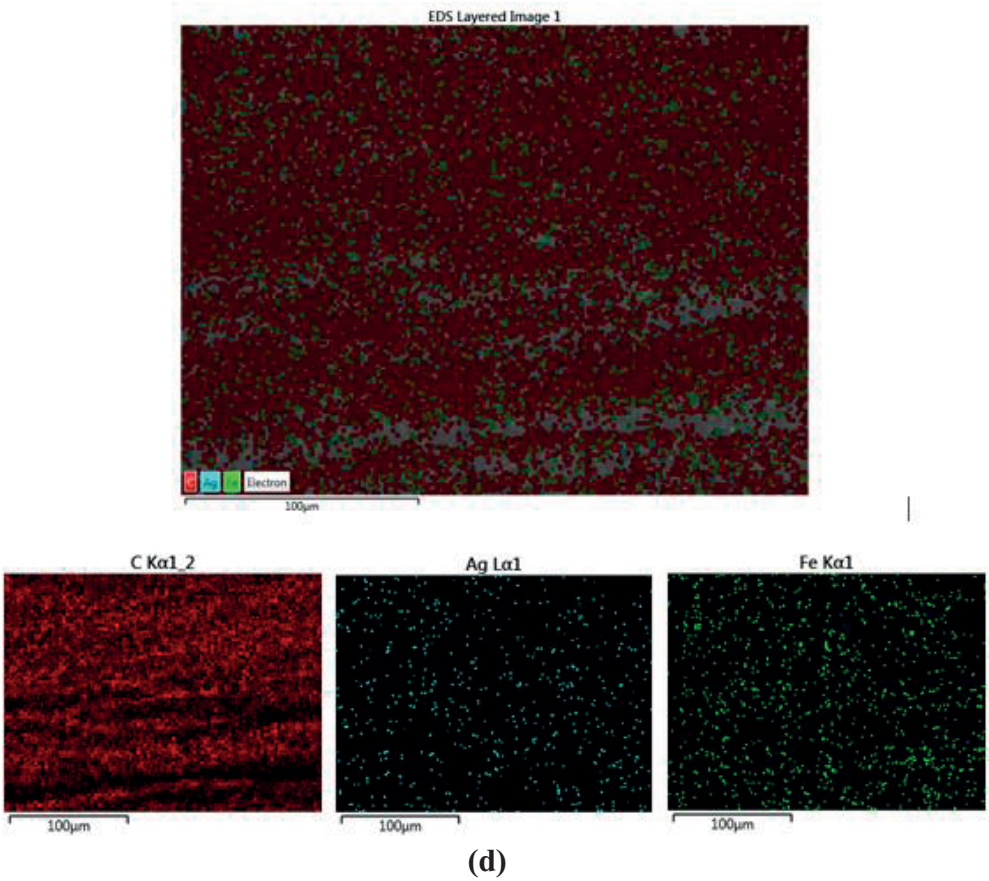

Figure 4. Continued.

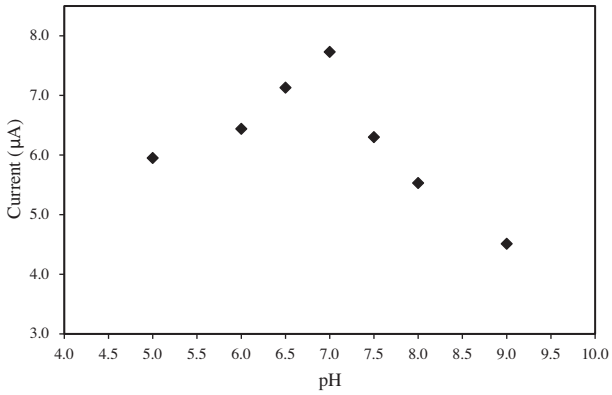

Figure 5. Influence of pH on the response of the Ag/PVF-modified electrode prepared under optimum conditions. (Data obtained from CVs of N_2-saturated PBS (pH = 7.0) in the presence of 1.0 mM H_2O_2.)

2.4. Chronoamperometry studies and amperometric detection of H_2O_2

Chronoamperometry is a useful method for determining the catalytic rate constant (k_{cat}) using the equation

$$I_{cat}/I_L = \pi^{1/2}(k_{cat}C_0t)^{1/2}, \quad (1)$$

where I_{cat} is the catalytic current of the Ag/PVF catalyst in the presence of H_2O_2, I_L is the limiting current in the absence of H_2O_2, C_0 is the bulk concentration of H_2O_2 (M), and t is the elapsed time (s).[53] For this purpose, we sketched I_{cat}/I_L versus $t^{1/2}$ using chronoamperometric data obtained from 10 mM solution of H_2O_2 at –0.5 V versus SCE (not shown). From the slope of I_{cat}/I_L versus $t^{1/2}$ plot, k_{cat} was 2.4 $\times$ 10^3 M^{-1} s^{-1}. This value is in the same order of magnitude with H_2O_2 sensors in the literature.[54,55]

Chronoamperometric data can also be used for estimation of the diffusion coefficient (D) for an electroactive material using Cottrell's equation:

$$I = nFAC(D/\pi t)^{1/2}, \tag{2}$$

where n is the number of electrons, F is the Faraday constant, A is the electrode area, C is the bulk concentration of the analyte, and t is the elapsed time.[56] In order to determine the specific surface area (A) of the Ag/PVF-modified Au electrode, cyclic voltammetry experiments were performed with the modified electrode in 1.0 mM $K_3[Fe(CN)_6]$ + 50 mM KCl at different scan rates (between 10 and 100 mV s^{-1}). From the slope of anodic peak current (I_{pa}) versus square root of scan rate ($v^{1/2}$) plot, the estimated value for A was calculated as 0.123 cm^2 using the following equation:

$$I_{pa} = (2.69 \times 10^5)n^{2/3}AD^{1/2}v^{1/2}C_0 \tag{3}$$

using 7.6 $\times$ 10^{-6} cm^2 s^{-1} as the diffusion coefficient for $K_3[Fe(CN)_6]$.[56,57] According to the chronoamperometric data of 10 mM H_2O_2 solution, the diffusion coefficient of H_2O_2 was 7.40 $\times$ 10^{-6}, which is reasonable compared with the literature.[53,58]

The performance of the Ag/PVF-modified Au electrode as an enzymeless amperometric H_2O_2 sensor was evaluated by chronoamperometry. Figure 6a shows the typical current–time curve of the sensor prepared under optimized conditions after successive additions of certain concentrations H_2O_2 to a continuously stirred N_2-saturated PBS solution (pH = 7.4). The applied potential was –0.5 V versus SCE. The results revealed that the sensor had a short response time (under 5 s) and was sensitive to the addition of H_2O_2 aliquots in a wide concentration range.

The calibration curve obtained from chronoamperometric data indicated a good linear relationship between the peak current and H_2O_2 concentration over a wide concentration range (0.1 to 50 mM) with a correlation coefficient of 0.9964 (Figure 6b). LOD was calculated as 0.94 μM according to Borgmann et al. (N = 6) with a signal-to-noise ratio of 3, which is lower than many of the previously reported sensors.[59] Sensitivity of the sensor was 14.1 μA mM^{-1}. As a comparison, analytical performances of some enzymeless H_2O_2 sensors based on Ag nanoparticles is presented in Table 1 in terms of LOD and linear range.

2.5. Interference study

The influence of common interfering species such as uric acid (UA), ascorbic acid (AA), dopamine (DA), and glucose (Glu) was investigated. As clearly seen in Figure 7, none of these species demonstrated a significant interference to the signal of 0.5 mM H_2O_2 at a concentration of 0.5 mM under optimum working conditions. Thus it can be concluded that H_2O_2 can be determined selectively with the prepared sensor in the presence of these interferents.

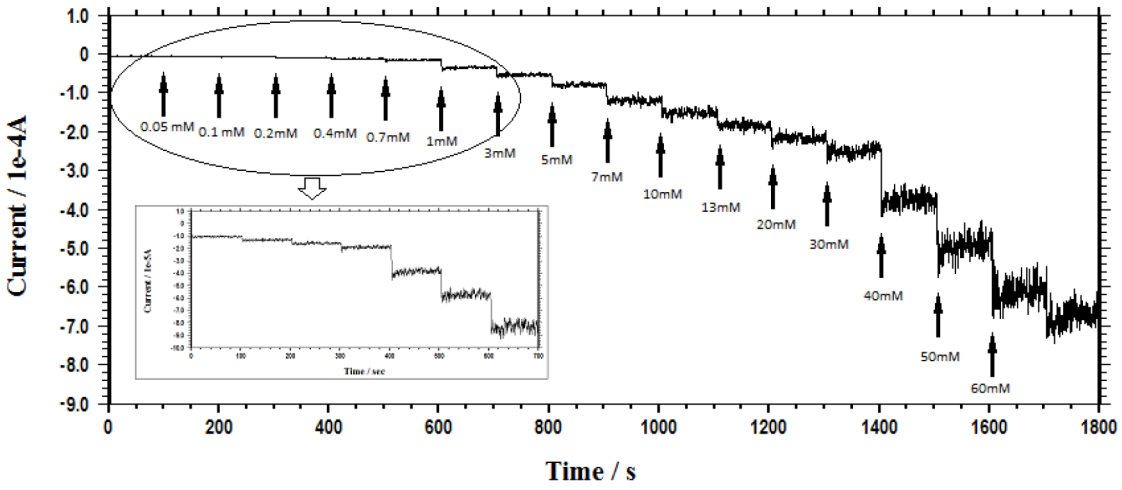

(a)

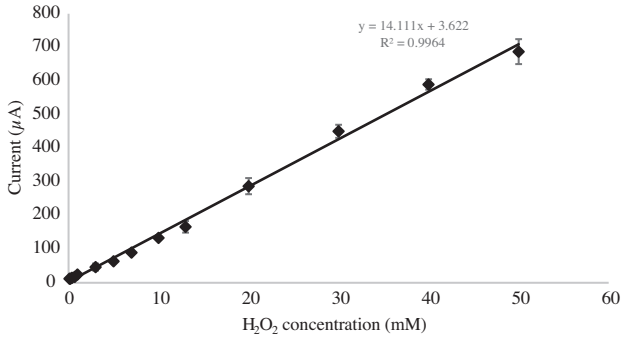

(b)

Figure 6. (a) Current–time responses of Ag/PVF-modified Au electrode to successive injections of H_2O_2 into 50 mM N_2-saturated PBS (pH = 7.4) at –0.5 V versus SCE. (b) The corresponding calibration curve.

2.6. Real sample analysis

The Ag/PVF-modified Au electrode was applied to the determination of H_2O_2 in hair dye oxidant cream. An oxidant cream sample (3.0 mL) with a reported H_2O_2 concentration of 9% (v/v) was diluted to 100 mL. From this solution, three different samples were prepared (1.0 mM, 5.0 mM, and 10.0 mM) and analyzed using standard addition. As seen from the analysis results in Table 2, the modified electrode presented a poor recovery (%) response for determination of H_2O_2 in concentrated real samples. However, in samples with moderate concentrations, the results indicate that the Ag/PVF-modified Au electrode is applicable for real sample analysis.

2.7. Reproducibility of Ag/PVF-modified Au electrode

In order to investigate the reproducibility of the Ag/PVF-modified Au electrode, reduction current obtained by chronoamperometry using 10 mM H_2O_2 solution was monitored daily for 10 days. When not in use, the modified electrode was kept at 4 °C, open to air, and no visual change was observed on the electrode surface. The current response was the same for the first two days and decreased gradually afterwards to 29% of the initial current in 10 days (Figure 8).

Table 1. Comparison between performances of different enzymeless H_2O_2 sensors containing Ag nanoparticles.

Modified electrode	LOD (μM)	Linear range (mM)	Reference
MWCNT/Ag nanohybrids/Au	0.5	0.05–17	[34]
Ag NPs/ZnO/GCE	0.42	0.002–5.5	[31]
AgNP/rGO/GCE	7.1	0.1–80	[35]
AgNP/F-SiO_2/GO/GCE	4	0.1–260	[36]
AgNPs/rGO/GCE	3.6	0.1–100	[20]
AgNP/TiO_2 NWs/GCE	1.70	0.1–60	[30]
AgNPs/rGO/GCE	1.80	0.1–60	[32]
Ag NW array	29.2	0.1–3.1	[19]
AgNPs/MWCNTs-IL/GCE	0.0039	1.2×10^{-5} – 4.8×10^{-3}	[21]
AgNP/rGO/GCE	10	0.05–5	[22]
AgNP-PmPD/GCE	0.88	0.1–10	[10]
AgNPs/Ox-pTTBA/MWCNT/GCE	0.24	0.010–0.260	[11]
Ag/PVF/Au	0.94	0.1–50	This work

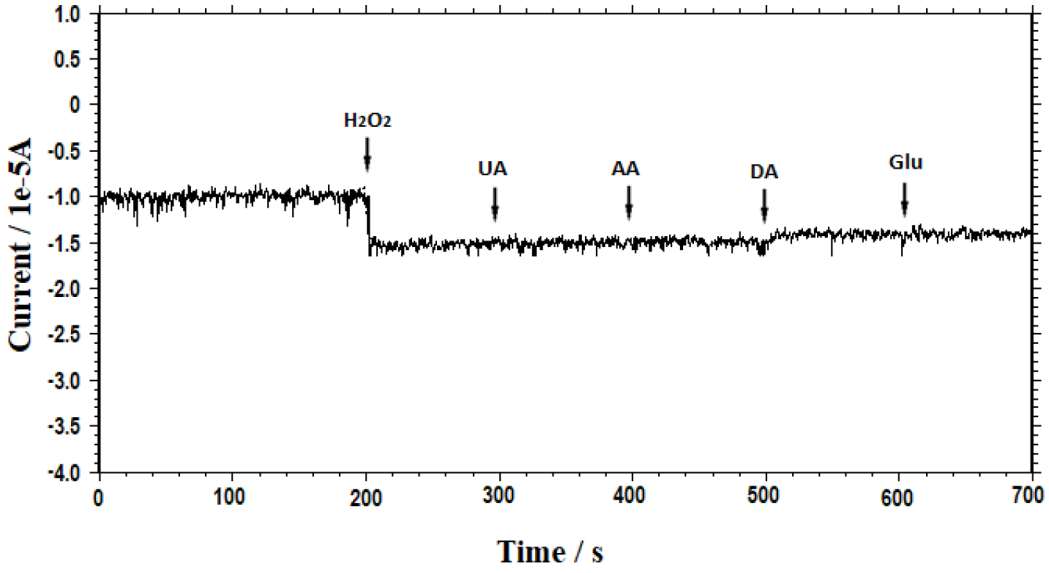

Figure 7. Current–time responses of Ag/PVF-modified Au electrode exposed to UA, AA, DA, and Glu (0.5 mM each) in the presence of 0.5 mM H_2O_2 at an applied potential of –0.5 V versus SCE.

Table 2. Determination of H_2O_2 in hair dye oxidant cream.

Sample	Added (mM)	Found (mM)	Recovery (%)	RSD (%, n = 3)
1	1.00	1.04	104.0	2.7
2	5.00	4.82	96.4	1.4
3	10.00	29.8	298.0	6.0

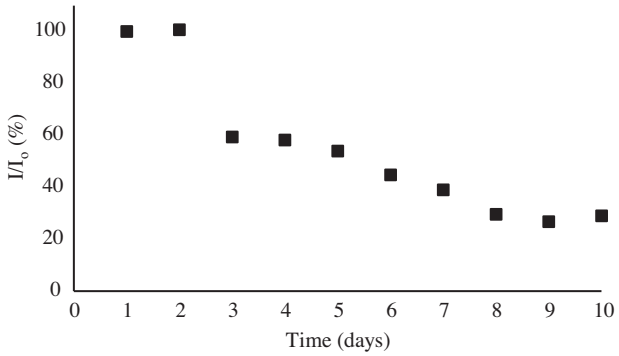

Figure 8. Reproducibility of Ag/PVF-modified Au electrode studied for 10 days.

2.8. Conclusions

A modified electrode system was developed based on Ag nanoparticles supported on conducting PVF film. As expected, the synergetic effect of combining PVF and the Ag nanoparticles resulted in enhanced sensor response even without using an enzyme for H_2O_2 detection. One of the most important features of the sensor is the ease of preparation, together with the low LOD compared with similar studies in the literature. The developed sensor exhibited a very good linearity within the concentration range of 0.1 mM to 50 mM, with a detection limit of 0.94 μM. Sensitivity of the sensor was calculated as 14.1 μA mM^{-1}. The interference study indicated that the enzymeless sensor was not affected by common interferents such as UA, AA, DA, and Glu. These characteristics make the Ag/PVF system an excellent amperometric sensor for detection of low levels of H_2O_2.

3. Experimental

3.1. Reagents and instruments

Poly(vinylferrocene) was synthesized according to the procedure described by Aso et. al.[60] Vinylferrocene was obtained from Sigma-Aldrich (St. Louis, MO, USA). 2,2-Azo-bis(2-methyl-propionitrile) was obtained from Alfa (Ronkonkoma, NY, USA). TBAP ($\geq$99.0%) was purchased from Fluka (Munich, Germany). Methylene chloride (HPLC grade) was obtained from Sigma-Aldrich. Hydrogen peroxide solution was diluted from 30% aqueous stock solution (Sigma-Aldrich). $AgNO_3$, NaH_2PO_4, Na_2HPO_4, UA, AA, and DA were purchased from Sigma-Aldrich and used as received.

All solutions were deoxygenated by purging high-purity nitrogen gas prior to use in the electrochemical experiments and all experiments were carried out at ambient temperature.

Electrochemical experiments were performed using a CHI 600E electrochemical workstation. SEM images were recorded using a JEOL model JSM-7001F (Tokyo, Japan).

3.2. Electrodes

Electrochemical experiments were carried out in a three-electrode system glass cell. A Au disc electrode (r = 1 mm) was used as the working electrode. This electrode was polished using alumina (first 1.0 μm, then 0.3 μm), then rinsed with triple-distilled water, cleaned in an ultrasonic bath, and dried. Ag/AgCl and SCE were used as reference electrodes in methylene chloride and aqueous media, respectively. A Pt wire was used as the counter electrode. In order to record SEM images, the PVF coating and the Ag/PVF catalyst system were prepared on disposable PGEs.

3.3. Preparation of the Ag/PVF-modified Au electrode

During the procedure, the polymer film was first deposited onto the working electrode by electrooxidation of 1.0 mg mL^{-1} PVF solution in methylene chloride containing 0.1 M TBAP as the supporting electrolyte. The potential was held constant at 0.7 V versus Ag/AgCl throughout the electrolysis. In the second step, the PVF-coated electrode was immersed in a stirred aqueous solution of $AgNO_3$ in order to immobilize the Ag^+ ions in the polymeric matrix. After this step, the electrode was washed thoroughly with triple-distilled water and placed in an electrochemical cell containing 50 mM phosphate buffer system (pH = 7.0) in order to reduce the Ag^+ ions at constant potential to obtain PVF-supported Ag nanoparticles.

Acknowledgment

This work was supported by the Scientific and Technological Research Council of Turkey (TÜBİTAK) with grant number 114Z685.

References

1. Chen, W.; Cai, S.; Ren, Q. Q.; Wen, W.; Zhao, Y. D. *Analyst* **2012**, *137*, 49-58.
2. Chen, S.; Yuan, R.; Chai, Y.; Hu, F. *Microchim. Acta* **2013**, *180*, 15-32.
3. Ramos, M. C.; Torijas, M. C.; Navas Diaz, A. *Sens. Actuators B Chem.* **2001**, *73*, 71-75.
4. Tahirovic, A.; Copra, A.; Omanovic-Miklicanin, E.; Kalcher, K. *Talanta* **2007**, *72*, 1378-1385.
5. Xu, C.; Zhang, Z. *Anal. Sci.* **2001**, *17*, 1449-1451.
6. Ling, Y.; Zhang, N.; Qu, F.; Wen, T.; Gao, Z. F.; Li, N. B.; Luo, H. Q. *Spectrochim. Acta A* **2014**, *118*, 315-320.
7. Tanner, P. A.; Wong, A. Y. S. *Anal. Chim. Acta* **1998**, *370*, 279-287.
8. Pappas, A. Ch.; Stalikas, C. D.; Fiamegos, Y. Ch.; Karayannis, M. I. *Anal. Chim. Acta* **2002**, *455*, 305-313.
9. Zhao, W.; Wang, H.; Qin, X.; Wang, X.; Zhao, Z.; Miao, Z.; Chen, L.; Shan, M.; Fang, Y.; Chen, Q. *Talanta* **2009**, *80*, 1029-1033.
10. Wu, Z.; Yang, S.; Chen, Z.; Zhang, T.; Guo, T.; Wang, Z.; Liao, F. *Electrochim. Acta* **2013**, *98*, 104-108.
11. Abdelwahab, A. A.; Shim, Y. B. *Sens. Actuators B Chem.* **2014**, *201*, 51-58.
12. Liu, C. Y.; Hu, J. M. *Biosens. Bioelectron.* **2009**, *24*, 2149-2154.
13. Yao, H.; Li, N.; Xu, S.; Xu, J. Z.; Zhu, J. J.; Chen, H. Y. *Biosens. Bioelectron.* **2005**, *21*, 372-377.
14. Eftekhari, A. *Talanta* **2001**, *55*, 395-402.
15. Liu S.; Dai, Z.; Chen, H.; Ju, H. *Biosens. Bioelectron.* **2004**, *19*, 963-969.
16. Şenel, M.; Çevik, E.; Abasıyanık, M. F. *Sens. Actuators B Chem.* **2010**, *145*, 444-450.
17. Chen, S.; Yuan, R.; Chai, Y.; Zhang, L.; Wang, N.; Li, X. *Biosens. Bioelectron.* **2007**, *22*, 1268-1274.
18. Luo, X.; Morrin, A.; Killard, A. J.; Smyth, M. R. *Electroanalysis* **2006**, *18*, 319-326.
19. Kurowska, E.; Brzozka, A.; Jarosz, M.; Sulka, G. D.; Jaskula, M. *Electrochim. Acta* **2013**, *104*, 439-447.
20. Li, Q.; Qin, X.; Luo, Y.; Lu, W.; Chang, G.; Asiri, A. M.; Al-Youbi, A. O.; Sun X. *Electrochim. Acta* **2012**, *83*, 283-287.
21. Li, X.; Liu, Y.; Zheng, L.; Dong, M.; Xue, Z.; Lu, X.; Liu, X. *Electrochim. Acta* **2013**, *113*, 170-175.
22. Wang, M. Y.; Shen, T.; Wang, M.; Zhang, D.; Chen, J. *Mater. Lett.* **2013**, *107*, 311-314.
23. Mahmoudian, M. R.; Alias, Y.; Basirun, W. J.; Ebadi, M. *Electrochim. Acta* **2012**, *72*, 46-52.

24. Zhang, Y.; Liu, Y.; He, J.; Pang, P.; Gao, Y.; Hu, Q. *Electrochim. Acta* **2013**, *90*, 550-555.
25. Narang, J.; Chauhan, N.; Pundir, C. S. *Analyst* **2011**, *136*, 4460-4466.
26. Li, X.; Liu, X.; Wang, W.; Li, L.; Lu, X. *Biosens. Bioelectron.* **2014**, *59*, 221-226.
27. Xu, F.; Sun, Y.; Zhang, Y.; Shi, Y.; Wen, Z.; Li, Z. *Electrochem. Commun.* **2011**, *13*, 1131-1134.
28. Chen, X. M.; Cai, Z. X.; Huang, Z. Y.; Oyama, M.; Jiang, Y. Q.; Chen, X. *Electrochim. Acta* **2013**, *97*, 398-403.
29. Hosseini, H.; Rezaei, S. J. T.; Rahmani, P.; Sharifi, R.; Nabid, M. R.; Bagheri, A. *Sens. Actuators B Chem.* **2014**, *195*, 85-91.
30. Qin, X.; Lu, W.; Luo, Y.; Chang, G.; Asiri, A. M.; Al-Youbi A. O.; Sun, X. *Electrochim. Acta* **2012**, *74*, 275-279.
31. Wang, Q.; Zheng, J. *Microchim. Acta* **2010**, *169*, 361-365.
32. Qin, X.; Luo, Y.; Lu, W.; Chang, G.; Asiri, A. M.; Al-Youbi, A. O.; Sun, X. *Electrochim. Acta* **2012**, *79*, 46-51.
33. Song, M. J.; Hwang, S. W.; Whang D. *J. Appl. Electrochem.* **2010**, *40*, 2099-2105.
34. Zhao, W.; Wang, H.; Qin, X.; Wang, X.; Zhao, Z.; Miao, Z.; Chen, L.; Shan, M.; Fang, Y.; Chen, Q. *Talanta* **2009**, *80*, 1029-1033.
35. Liu, S.; Wang, L.; Tian, J.; Luo, Y.; Zhang, X.; Sun, X. *J. Colloid Interface Sci.* **2011**, *363*, 615-619.
36. Lu, W.; Luo, Y.; Chang, G.; Sun, X. *Biosens. Bioelectron.* **2011**, *26*, 4791-4797.
37. Zhang, S.; Liu, X.; Huang, N.; Lu, Q.; Liu, M.; Li, H.; Zhang, Y.; Yao, S. *Electrochim. Acta* **2016**, *211*, 36-43.
38. Nia, P. M.; Meng, W. P.; Alias, Y. *Appl. Surf. Sci.* **2015**, *357*, 1565-1572.
39. Azizi, S. N.; Ghasemi, S.; Samadi-Maybodi, A.; Ranjbar-Azad, M. *Sens. Actuators B Chem.* **2015**, *216*, 271-278.
40. Ensafi, A. A.; Rezaloo, F.; Rezaei, B. *Sens. Actuators B Chem.* **2016**, *231*, 239-244.
41. Gündoğan-Paul, M.; Özyörük, H.; Çelebi, S. S.; Yıldız, A. *Electroanalysis* **2002**, *14*, 505-511.
42. Gündoğan-Paul, M.; Çelebi, S. S.; Özyörük, H.; Yıldız, A. *Biosens. Bioelectron.* **2002**, *17*, 875-881.
43. Aydın, G.; Çelebi, S. S.; Özyörük, H.; Yıldız, A. *Sens. Actuators B Chem.* **2002**, *87*, 8-12.
44. Kuralay, F.; Özyörük, H.; Yıldız, A. *Sens. Actuators B Chem.* **2005**, *109*, 194-199.
45. Kuralay, F.; Özyörük, H.; Yıldız, A. *Sens. Actuators B Chem.* **2006**, *114*, 500-506.
46. Topçu Sulak, M.; Gökdoğan, Ö.; Gülce, A.; Gülce, H. *Biosens. Bioelectron.* **2006**, *21*, 1719-1726.
47. Özer, B. C.; Özyörük, H.; Çelebi S. S.; Yıldız A. *Enzyme Microb. Technol.* **2007**, *40*, 262-265.
48. Gökdoğan Şahin, Ö.; Gülce, H.; Gülce, A. *J. Electroanal. Chem.* **2013**, *690*, 1-7.
49. Türkmen, E.; Baş, S. Z.; Gülce, H.; Yıldız, S. *Electrochim. Acta* **2014**, *123*, 93-102.
50. Peerce, J. J.; Bard, A. J. *J. Electroanal. Chem.* **1980**, *112*, 97-115.
51. Sönmez Çelebi, M.; Pekmez, K.; Özyörük, H.; Yıldız, A. *J. Power Sources* **2008**, *183*, 8-13.
52. Sönmez Çelebi, M.; Özyörük, H.; Abacı, S. *Hacettepe Journal of Biology & Chemistry* **2014**, *42*, 569-576.
53. Shamsipur, M.; Karimi, Z.; Tabrizi, M. A. *Mater. Sci. Eng. C* **2015**, *56,* 426-431.
54. Pandey, P. C.; Pandey, A. K. *Electrochim. Acta* **2013**, *87*, 1-8.
55. Salazar, P.; Martín, M.; O'Neill, R. D.; Roche, R.; González-Mora, J. L. *J. Electroanal. Chem.* **2012**, *674*, 48-56.
56. Bard, A. J.; Faulkner, L. R. *Electrochemical Methods Fundamentals and Applications*; Wiley: New York, NY, USA, 2001.
57. Siswana, M. P.; Ozoemena, K. I.; Nyokong, T. *Electrochim. Acta* **2006**, *52,* 114-122.
58. Hasheminejad, E.; Raoof, J. B.; Ojani, R.; Nadimi, S. R. *J Iran. Chem. Soc.* **2015**, *12*, 2037-2044.
59. Borgmann, S.; Schulte, A.; Neugebauer, S.; Schuhmann, W. *Advances in Electrochemical Science and Engineering*; Wiley-VCH: Weinheim, Germany, 2011.
60. Aso, C.; Kunitake, T.; Nakashima, T. *Macromol. Chem.* **1969**, *124*, 232-239.